

See discussions, stats, and author profiles for this publication at: <http://www.researchgate.net/publication/281966130>

One-step continuous extrusion process for the manufacturing of solid dispersions

ARTICLE *in* INTERNATIONAL JOURNAL OF PHARMACEUTICS · SEPTEMBER 2015

Impact Factor: 3.65 · DOI: 10.1016/j.ijpharm.2015.09.048

READS

31

6 AUTHORS, INCLUDING:



Mohammed Maniruzzaman

University of Greenwich

31 PUBLICATIONS **190** CITATIONS

SEE PROFILE



Nikolaos Scoutaris

University of Greenwich

11 PUBLICATIONS **86** CITATIONS

SEE PROFILE



Dennis Douroumis

University of Greenwich

67 PUBLICATIONS **542** CITATIONS

SEE PROFILE

Accepted Manuscript

Title: One-step continuous extrusion process for the manufacturing of solid dispersions

Author: M. Maniruzzaman A. Nair N. Scoutaris Michael S.A. Bradley M.J. Snowden D. Douroumis



PII: S0378-5173(15)30249-0
DOI: <http://dx.doi.org/doi:10.1016/j.ijpharm.2015.09.048>
Reference: IJP 15233

To appear in: *International Journal of Pharmaceutics*

Received date: 18-7-2015
Revised date: 17-9-2015
Accepted date: 19-9-2015

Please cite this article as: Maniruzzaman, M., Nair, A., Scoutaris, N., Bradley, Michael S.A., Snowden, M.J., Douroumis, D., One-step continuous extrusion process for the manufacturing of solid dispersions. *International Journal of Pharmaceutics* <http://dx.doi.org/10.1016/j.ijpharm.2015.09.048>

This is a PDF file of an unedited manuscript that has been accepted for publication. As a service to our customers we are providing this early version of the manuscript. The manuscript will undergo copyediting, typesetting, and review of the resulting proof before it is published in its final form. Please note that during the production process errors may be discovered which could affect the content, and all legal disclaimers that apply to the journal pertain.

One-step continuous extrusion process for the manufacturing of solid dispersions

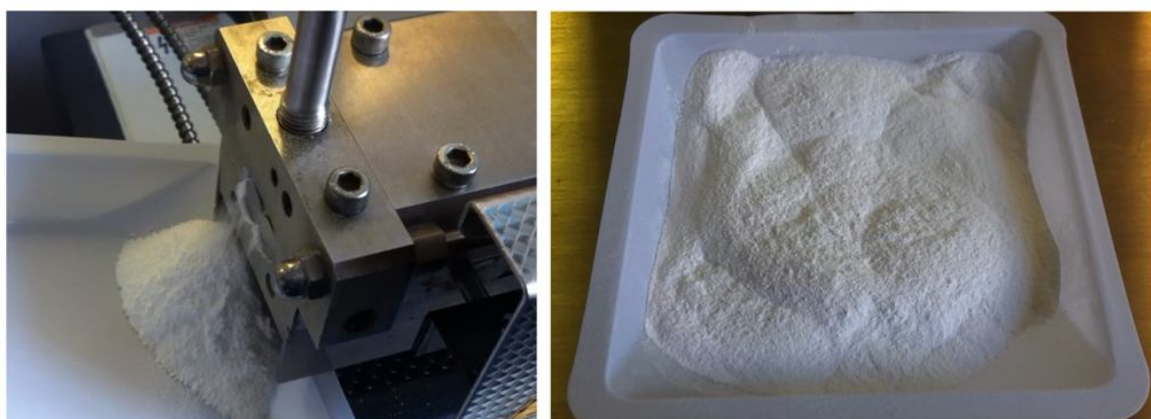
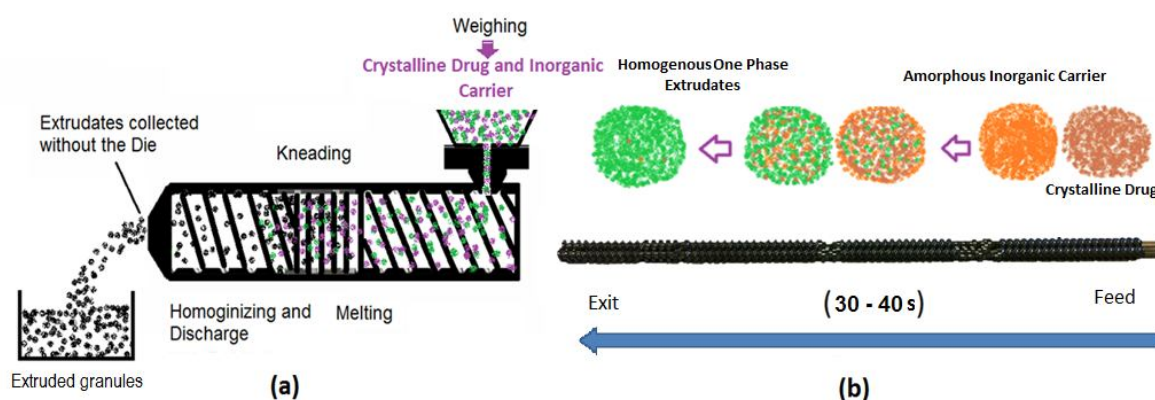
M. Maniruzzaman¹, A. Nair², N. Scoutaris¹, Michael S.A. Bradley³, M. J. Snowden¹, D. Douroumis¹

¹Faculty of Engineering and Science, School of Science, University of Greenwich, Chatham Maritime, Chatham, Kent ME4 4TB, UK

²Fuji Chemical Industry Co., Ltd., 12F The Front Tower Shiba Koen, 2-6-3 Shibakoen, Minato-Ward, Tokyo, 105-0011 Japan

³The Wolfson Centre for Bulk Solids Handling Technology, Medway School of Engineering, University of Greenwich, Medway Campus, Chatham Maritime, Kent, UK

Graphical abstract



(c)

Abstract

The purpose of this study was to evaluate the performance of synthetic magnesium aluminometasilicate (MAS) as a novel inorganic carrier in hot melt extrusion (HME) processing of indomethacin (IND) for the development of solid dispersions. A continuous extrusion process at various IND/excipient blend ratios (20%, 30% and 40%) was performed using a twin - screw extruder. Physicochemical characterisation carried out by SEM, DSC, and XRPD demonstrated the presence of IND in amorphous nature within the porous network of the inorganic material for all extruded formulations. Further, AFM and FTIR studies revealed a single-phase amorphous system and intermolecular H-bonding formation. The IND/MAS extrudates showed enhanced INM dissolution rates within 100% been released within 1 hr. Stability studies under accelerated conditions (40°C, RH 75%) showed that MAS retained the physical stability of the amorphous solid dispersions even at high drug loadings for 12 months.

Key Words: inorganic excipients, solid dispersions, continuous extrusion

1.0 INTRODUCTION

The increasing number of new lead compounds that fail out in the discovery pipeline due to their poor water solubility is considered one of the major challenges in pharmaceutical formulation development. Therefore, there is a growing interest to improve the aqueous solubility and thus the oral bioavailability of those poorly water-soluble drugs for the development of oral dosage forms (Maniruzzaman et al., 2012). Several processing techniques have been utilized to improve drug solubility such as size reduction, hot spin mixing (Srinarong et al., 2011), spray drying (Alam et al., 2012, Jang et al., 2013), co-evaporation or co-precipitation (Kushida et al., 2013), freeze-drying (He et al., 2011), supercritical fluid processing (SFP) (Gong et al., 2005) and recently hot-melt extrusion (HME) (Maniruzzaman et al., 2013a, 2013b). HME has been used as a processing technology in order to enhance the dissolution rates of poorly soluble drugs by producing solid dispersions. It is a solvent free, dust-free, environmentally friendly, easy to scale up and can

be used as a continuous manufacturing process. HME has demonstrated its processing capability to develop various solid dosage forms such as pellets capsules, films or tablets (Maniruzzaman et al., 2013b, Repka et al., 2008, 2012, Gryczke et al., 2011, Lang et al., 2014, Repka et al., 2012a). Generally, the high shear force generated inside the extruder barrel and the optimised processing parameters (e.g. screw speed, feed rate, temperatures) during the HME process, are applied to overcome the crystal lattice energy of crystalline drugs and soften the carrier matrices. Up to date, most of these studies investigated the use of hydrophilic polymers or lipids as carrier matrices to develop solid dispersions (Maniruzzaman et al., 2013b, Repka et al., 2012b).

The use of inorganic excipients (Gupta et al., 2002) as drug carriers for increase dissolution rates of poorly water-soluble drugs is an attractive approach which can provide a new insight into pharmaceutical research and product development.

Bahl *et al.*, reported the effects of magnesium aluminometasilicate (MAS) as a novel inorganic excipient on the increase of amorphicity of indomethacin (BCS class II drug) in a mechanical ball milling process and thus enhancing its dissolution rates (Bahl and Bogner, 2006). Later on the same group reported a follow up study evaluating the solubility and dissolution profiles of indomethacin (both crystalline and amorphous state) in the presence of MAS as an inorganic carrier (Bahl and Bogner, 2008) via a ball milling process. The presence of silicic acid and Mg^{2+}/Al^{3+} ions, from the MAS molecule, in the dissolution media was found to cause the increase in the concentration of indomethacin and enhance its *in vitro* dissolution rates.

Maclean *et al.*, proposed a scalable process to form a Sulindac-MAS amorphous drug complex using a twin screw granulation approach (Maclean et al., 2011). The dissolution properties of the resulting melt extruded material was improved while maintaining similar physical stability as those manufactured in ball milling.

MAS is an amorphous magnesium aluminometasilicate with a high specific surface area ($300\text{ m}^2/\text{g}$) (Fuji Chemical Industry Co., Ltd., 2015). Like many silicates, MAS generates different silanol types (e.g. free, germinal or associated) in contact with water, which make it a potential proton donor as well as a proton acceptor. MAS also presents exceptional excipients properties such as high flowability, high surface area, porous, thermal and mechanical stability for improved API delivery and the quality of pharmaceutical dosage forms. Indomethacin is a BCS class II drug with low solubility and high permeability which has been previously processed by HME for the development of polymeric solid dispersion

either in amorphous state or molecularly dispersed (Maniruzzaman et al., 2013, Chokshi et al., 2008).

The aim of the current study was to utilize inorganic excipients as drug carriers for the manufacturing of solid dispersions of water insoluble drugs with increase dissolution rates. HME was used a continuous one step extrusion process of drug – inorganic excipient blends at various IND loadings.

2. MATERIALS AND METHOD

2.1 Materials

Indomethacin ($\geq 98\%$) was purchased from Tokio Chemical Industries (Belgium) and magnesium aluminometasilicate (MAS-Neusilin® US2) ($\geq 99\%$) was kindly donated by Fuji Chemical Industries Co., Ltd. (Japan). All solvents used were of analytical grade and used as received.

2.2 Hot-melt extrusion processing

All prepared binary mixtures were extruded without the die at temperatures varying from 170 – 200°C to find the suitable extrusion temperatures. The extrusion was conducted in a twin screw (co-rotating) extruder with an L/D ratio 40:1 (ThermoFisher, Germany). The temperatures profiles were finally optimized using 50/100/180/180/180/180/180/180/180/25°C (feeder – die) with a screw speed of 100 rpm and the feed rate of 1 kg/hr. The feeding was optimized using a volumetric feeder equipped with single screw (Brabender, Germany). The temperatures, screw speed and the torque forces were recorded for each processed batch. Three different formulations with IND/MAS 20/80, 30/70 and 40/60 (% w/w) were used for extrusion in order to obtain the final extrudates as free flowing granules. The specific ratios of drug/excipients were chosen based on the dose of marketed indomethacin. Moreover a wide range of the drug loadings from 20 to 40% w/w ratios was investigated in order to develop amorphous solid dispersions and thus enhancing the dissolution of poorly soluble drug. No additional down streaming processing was required to micronize the particle size of the extrudates.

2.3 Residence time distribution and mean residence time measurement

The residence time (t) distribution (RTD) was measured by adding 0.5 g of Indigo Carmine (FDA approved food colorant with melting point $>300^\circ\text{C}$) pigment as a tracer to the

hopper of the feeding section at a given time T_0 . The colour concentration of the extruded granules was measured via a UV spectrophotometer set at wavelength 620 nm at the die. The sampling time intervals were set at 2 s. All obtained absorbance values from the coloured extrudates were used to plot a graph of Absorbance Vs Time to determine the residence time distribution ($n=3$).

The mean residence time (t') for all extruded formulations was measured by using the following equation (Eq. 1) (Hasan et al., 2013, Koltuniewicz and Noworyta, 1994, Levenspiel, 1972):

$$t' = \frac{\sum_0^{\infty} tC\Delta t}{\sum C\Delta t} \quad (1)$$

Where, C is the measured concentration in the UV spectrophotometer, Δt is the time difference. By using the calculated t' , the variance in the residence time distribution was also determined.

2.4 Scanning electron microscopy (SEM)

SEM was used to study the surface morphology of the hot-melt extrudates. The samples ($n=1$) were mounted on an aluminium stage using adhesive carbon tape and placed in a low humidity chamber prior to analysis. Samples were coated with gold, and microscopy was performed using a Cambridge Instruments (S630, UK), SEM operating at an accelerating voltage of 5 kV.

2.5 Particle size analysis

The particle size distribution of the extrudates for all formulations was measured by dry sieving. The method involved stacking of the sieves on top of each other and then placing the test granules (~500 mg) on the top sieve ($n=3$). The nest of sieves was subjected to a standardised period of agitation (2-4 min) and then the weight of the material retained on each sieve was accurately determined to give the weigh percentage of granules in each sieve size range.

2.6 Atomic Force Microscopy (AFM)

AFM analysis was performed on tapping mode using an easyscan 2 (nanosurf, Switzerland). Tap 190Al-G cantilevers were used (BudgetSensors, Sofia, Bulgaria). The drive amplitude and the relative set point were chosen in a way that the intermittent force between the oscillated tip and the substrate would be minimum. The analysis of the images was performed using SPIP software (Image Metrology, Hørsholm, Denmark).

2.7 X-ray powder diffraction (XRPD)

XRPD was used to determine the solid state of pure active substances, physical mixtures and extruded materials using a Bruker D8 Advance (Germany) in theta-theta mode. For the study purposes a Cu anode at 40 kV and 40 mA, parallel beam Goebel mirror, 0.2 mm exit slit, LynxEye Position Sensitive Detector with 3° opening (LynxIris at 6.5 mm) and sample rotation at 15 rpm were used. Each sample was scanned from 2 to 40° 2 θ with a step size of 0.02° 2 θ and a counting time of 0.1 seconds per step; 176 channels active on the PSD making a total counting time of 35.2 seconds per step.

2.8 Differential scanning calorimetry (DSC) study

A Mettler-Toledo 823e (Greifensee, Switzerland) differential scanning calorimeter (DSC) was used to carry out DSC runs of pure actives, physical mixtures and extrudates. About 2-5 mg of sample was placed in sealed aluminium pans with pierced lids. The samples were heated at 10°C/min from 0°C to 220°C under dry nitrogen atmosphere and reheated at the same heating rate.

In addition, modulated temperature differential scanning calorimetry (MTDSC) studies were performed from 25°C to 200°C with an underlying heating rate of 2°C/min. The pulse height was adjusted to 2°C with a temperature pulse width of 15-30 s.

2.9 Fourier Transform Infra-Red spectroscopy (FTIR)

FTIR analysis was performed on the drug, carrier, drug/carrier physical mixtures, and complex using Perkin Elmer PE1600 (Massachusetts 02451 USA) Fourier Transform Infrared Spectra according to the KBr disc method from 400 – 3600 wavelength/cm⁻¹ range.

2.10 *In vitro* dissolution study

In vitro drug release studies of the extruded granules (100 mg dosage) were carried out in 900 ml of 0.2 M dihydrogen-sodium-orthophosphate (pH adjusted with NaOH to 7.2)

for 2 hr using a Varian 705 DS dissolution paddle apparatus (Varian Inc. North Carolina, US) at 100 rpm (US Pharmacopeia, 2015a). All extruded granules were directly dropped in the vessels without filling them in a capsule (n=3). Dissolution bath and vessels were then equilibrated to $37 \pm 0.5^\circ\text{C}$. At predetermined time intervals, samples were withdrawn for HPLC assay. All dissolution studies were performed in triplicate.

2.11 HPLC analysis

The release of IND was determined by using HPLC, Agilent Technologies system 1200 series. A HYCHROME S50DS2-4889 ($5 \mu\text{m} \times 150 \text{ mm} \times 4 \text{ mm}$) column was used for the HPLC analysis of IND. The wavelength was set at 260 nm. The mobile phase consisted of methanol/water/acetic acid (64/35/1 v/v) and the flow rate was maintained at 1.5 ml/min and the retention time was 4-5 min. Calibration curve was prepared with concentrations varying from $10 \mu\text{g/ml}$ to $50 \mu\text{g/ml}$ and $20 \mu\text{l}$ injection volumes.

2.12 Stability studies

The extruded formulations were stored at 40°C and 75% relative humidity according to the ICH guidelines. The relative humidity was created with supersaturated solution of sodium chloride (Sigma Aldrich, Gillingham, UK). The extruded granules were placed in both open and closed glass vials prior to exposing in the pre-equilibrated accelerated conditions.

3. RESULTS AND DISCUSSION

3.1 Extrusion processing and RTD measurement

To find out the optimum processing parameters during melt extrusion process various IND/MAS ratios were processed at different extrusion temperatures ranging from $170\text{--}200^\circ\text{C}$. Based on the solid-state analysis (see below), it was found that temperatures above 180°C are suitable for the processing of IND/MAS batches as the crystalline IND was converted to its metastable form. As shown in Fig.1 the extrusion processing of MAS facilitated a complete dry blending with IND and free flowing granules were received. MAS is a suitable drug carrier for extrusion processing due to its high flowability (Carr's index 13), high specific surface area and the presence of Al_2O_3 (~30%). It has been reported that the Al_2O_3 either as tetrahedron or octahedron shape in MAS are randomly attached to form a complex three-dimensional structure, which may play a key role to the possible proton donor or acceptor capacity of the amorphous MAS. Moreover, the unique structural orientation in MAS does

not possess repeating units of a defined monomer making it an ideal carrier molecule to interact a wide range of drugs (Fuji Chemical Industry Ltd., 2015).

The excellent flowability of the extruded granules was also observed even at 40% drug loadings despite the sticky nature of IND. The estimated Carr's index values of IND/MAS (20-40%) extruded granules varied from 10-10.5 that is similar to bulk MAS. This optimized processing technology eliminates the downstream processing during the melt extrusion and it can provide several advantages such as low production cost, high throughput, less complex scale – up and reduced time to market during the pharmaceutical product manufacturing and development..

As shown in Fig. 2 at constant feed rate and screw speed the residence time distribution (RTD) determined for all formulations was narrow. The results showed that the time taken for the tracer to evacuate the extruder barrel from the point of feeding (T_0) is 35 s while the mean residence time was estimated at 40.0 s at 100 rpm and a constant feed rate of 1kg/h.

3.2 Particle morphology

SEM was used to examine the surface morphology of bulk IND and the extruded formulations. As it can be seen in Fig. 3a for all of the IND/MAS no drug crystals can be observed on the MAS surface suggesting excellent mixing and drug adsorption into the porous MAS network during processing. It can also be seen that IND/MAS granules appear as agglomerates of nanostructured particles. The formation of such extrudates with complete drug adsorption and reduced granular particle size during extrusion can be of great interest for the development of oral dosage forms. The foregoing claims are particularly of interests to particle engineering and thus dissolution enhancement of poorly water-soluble drugs. As it has been described before, that the smaller the particle size, the higher the surface area and thus higher the dissolution rates (Sun et al., 2012).

As shown in Fig. 3b the particle size distribution was determined for all extruded formulations and bulk MAS. A particle size reduction can be observed for the extruded formulations compared to bulk MAS with particle sizes varying from 40 – 300 μ m ($d(0.9) = 300\mu$ m). Interestingly, the application of high extrusion temperatures did not result in the formation of aggregates with large particle size and thus no further micronization was required.

3.3 Atomic force microscopy (AFM)

AFM was applied as a complementary technique to investigate whether IND has been dispersed/entrapped in matrices of inorganic MAS. The AFM images of IND/MAS extruded formulations are illustrated in Fig. 4. The phase images in showed that there is no phase separation between the components indicating that IND has been adsorbed by the MAS particles (Gupta et al., 2003). Moreover, there was no sign of crystallisation on the surface which also indicates the presence of IND in amorphous state within the inorganic excipient. Fig. 4 t also indicates that a homogenous dry blending was performed during the one-step HME processing which could be due to the entrapment of the IND particles inside the porous network of MAS. The observed results were consistent with all drug/excipient extruded formulations suggesting that even at high drug loading HME processing resulted in a one phase homogenous solid dispersions.

3.4 X-ray powder diffraction (XRPD)

X-ray analysis of bulk IND, physical mixtures and the IND/MAS extrudates, was conducted in order to examine IND crystalline state. As can be seen in Fig. 5 (inset), the diffractogram of pure IND presented distinct intensity peaks at 10.17, 11.62, 17.02, 19.60, 21.82, 23.99, 26.61, 29.37, 30.32, 33.55 2θ . The physical mixtures of all IND formulations showed identical peaks at lower intensities suggesting that the drug retains its crystallinity at loads of 20 – 40%. In contrast, no distinct intensity peaks were observed in the diffractograms of the extruded formulations even at high drug loadings. The absence of IND intensity peaks indicates the presence of IND in amorphous state within the MAS matrix.

3.5 Differential scanning calorimetry (DSC) and Modulated DSC

DSC was used to investigate the state of IND within the extruded formulations and compared with the physical mixtures (Table 1). As shown in Table 1, the DSC thermograms of pure IND showed sharp melting endothermic peak at 161°C with a fusion enthalpy (ΔH) of 100.88 J/g (Supp. Fig. 2). The analysis of the total heat flow of the bulk MAS (Supp. Fig 2) showed no crystalline melting peak but a sharp non reversible thermal transition due to the enthalpy relaxation at 161.70°C with a fusion enthalpy of 76.72 J/g (Bahl and Bogner, 2006, 2008). A further investigation with MTDSC showed the absence of the thermal transition at 161.70°C in the reversible heat flow indicating the transition due to a nonreversible enthalpy relaxation (data not shown).

As mentioned above, the suitable extrusion temperatures were based on the results obtained from the thermal analysis. As shown in supplementary material (Fig. S1) IND was

fully transformed to its amorphous form at processing temperatures above 180°C. In contrast extrudates processed at 160-170°C showed the presence of crystalline IND with a broad melting endotherm. Thus barrel temperature profiles above 180°C were used for processing of all IND/MAS optimized batches.

As can be seen in Fig. 6 all drug – excipient physical mixtures exhibited IND melting peaks at lower temperatures (150-155°C) with reduced enthalpy values as the ratio of carrier increased. However, the DSC thermograms for all IND/MAS 20-50% extruded formulations showed no endothermic peaks corresponding to the melting of IND (Fig. 6a) suggesting that the drug is dispersed in the MAS porous network in amorphous or molecularly dispersed state.

As it has been reported previously (Gupta et al., 2003), the electrostatic forces between the COO- group of IND and the counterions such as Mg²⁺ and Al³⁺ from MAS as well as the hydrogen- bonding interactions seemed to have driven the amorphization of the drug in the present study. It was also reported that the stronger the electrostatic interactions between the carboxylate group of IND and counterions, the higher the glass transition temperature of the amorphous materials. In our case, both the DSC and MTDSC couldn't determine the T_g of the amorphous MAS-bound drugs from a heating cycle 25-220°C. This could be attributed to the fact that the T_g may very well be higher than the melting point of the drugs itself. However, there are also similar reports where acid drugs were encapsulated in mesoporous silica carriers with similar thermal behaviour (Mellaerts et al., 2008a,b). In these particular cases the absence of any drug glass transition was justified by the strong drug interactions with inorganic excipient and the drug was considered molecularly dispersed.

3.6 FTIR analysis

IND exists as dimers in the crystalline state due to benzoyl carbonyl and carboxylic acid containing structure. The FTIR spectra (Fig. 7a, b) of the crystalline IND showed characteristic peaks at 1718 and at 1690 cm⁻¹, corresponding to the dimer carbonyl group and to the benzoyl carbonyl group respectively (Gupta et al., 2003). As shown in Fig. 7a, the absorbance peaks of the drug dimer disappeared in all extruded formulations, and a new peak appeared slightly shifted at 1685cm⁻¹. This phenomenon can be justified if the acidic nature of indomethacin due to its dimer carboxylic group is considered. Previous research showed that acidic drugs can interact with MAS as acid – base interaction. More specifically, Watanabe et al. reported that the pK_a values of SiO₂ and indomethacin are so close that a silanol group may become amphoteric, functioning as a Bronsted acid or as a Bronsted base. Therefore, due to the

local electronegativities of -COOH of IND and -Si-OH of SiO₂ the following bonding is formed -C-O-Si

Moreover, MAS is an amorphous magnesium aluminosilicate (MgO.Al₂O₃.SiO₂) a much more complex molecule than SiO₂ and hence it may be that the OH groups associated with Si, Mg, and Al in MAS have different acidic and basic strengths (Tong et al., 2002).

As expected in an acid–base reaction, the free acid carbonyl peak and the drug dimer or oligomer peaks disappeared and the peak for the carboxylate ion appeared. The presence of a carboxylate ion shows a strong peak in the region 1540–1650 cm⁻¹ in the FTIR spectrum.

3.7 *In vitro* dissolution studies

The main aim of the study was to develop IND/MAS extruded solid dispersion with increased dissolution rates. In Fig. 8 (i-ii), it can be seen that extrudates of 20 and 30% loadings of extruded IND/NEU provided rapid release of IND (100% in 60 min at pH 7.2) complying with USP monograph for IND (US Pharmacopeia, 2015b) while the physical mixture of all drug/polymer ratios showed relatively slower release compared to that of extrudates, however, slightly faster than the pure IND itself. As expected the release profiles of three different extruded formulations were identical. In addition it was observed that increased IND loading (40%) provided slightly slower release rates in contrast to the 20-30% loadings which could be due to the recrystallization of IND in the dissolution medium. Similar results were reported by Alonzo et al., (2010) where the authors found that amorphous indomethacin crystallized in an aqueous environment resulting the dissolution in supersaturated solutions. The reported crystallization from these supersaturated solutions was rapid. Nevertheless, the HME extruded formulations showed excellent release patterns that could provide fast onset action in future clinical trials.

3.8 Stability studies

All extruded formulations were investigated for their stability under accelerated conditions (40°C, 40% RH) for over 12 months. The samples were analysed with XRPD in order to identify any drug recrystallization and

The results obtained from the stability study under accelerated conditions showed that the use of MAS as drug carrier retained IND in amorphous state after 6 months storage for all drug loadings (20-40%). In addition no changes were observed in the dissolution profiles (Supp. Fig. 4). The XRPD data (Supp. Fig. 5) showed that all formulations were amorphous and stable in both open and closed conditions as no IND intensity peaks were observed. The

improved physical stability of the extruded solid dispersions could be attributed to their strong H-bonding interactions facilitated during the extrusion which maintain the stability for prolonged period of time.

4. Conclusions

In the current study MAS was exploited as a suitable carrier for continuous extrusion processing to manufacture amorphous solid dispersions of the poorly water-soluble indomethacin. IND was found molecularly dispersed in the porous network of the inorganic carrier and FTIR analysis showed the existence of the intermolecular H-bonding interactions between the IND carboxylic groups and the oxygen atoms of the carrier. *In vitro* dissolution studies revealed a significant increase of the dissolution rates of poorly water soluble IND. The extruded solid dispersions demonstrated excellent flowability and physical stability under accelerated conditions without any changes in IND crystallinity or dissolution rates. In conclusion, inorganic excipients (MAS) can be successfully used as carriers to manufacture amorphous solid dispersions, in the form of granules, with enhanced dissolution rates of poorly water soluble drugs.

Acknowledgements

The authors would like to thank Fuji Chemical Industry Co., Ltd., Japan for the financial contribution.

5.0 References

- Alam, M.A., Ali, R., Al-Jenoobi, F.I., Al-Mohizea, A.M., 2012. Solid dispersions: a strategy for poorly aqueous soluble drugs and technology updates. *Expert Opin Drug Deliv* 9, 1419-40.
- Alonzo, D. E., Zhang, G. G. Z., Zhou, D., Gao, Y., Taylor, L.S., 2010. Understanding the Behavior of Amorphous Pharmaceutical Systems during Dissolution. *Pharm Res* 27 (4), 608-618.
- Bahl, D., and Bogner, R. H., 2006. Amorphization of Indomethacin by Co-Grinding with Neusilin US2: Amorphization Kinetics, Physical Stability and Mechanism. *Pharm Res* 23, 2317-25.
- Bahl, D., and Bogner, R.H., 2008. Amorphization Alone Does Not Account for the Enhancement of Solubility of Drug Co-ground with Silicate: The Case of Indomethacin. *AAPS PharmSciTech* 9, 146-153.

- Chokshi, R.J., Shah, N.H., Sandhu, H.K., Malick, A.W., Zia, H., 2008. Stabilization of Low Glass Transition Temperature Indomethacin Formulations: Impact of Polymer-Type and Its Concentration. *J Pharm Sci* 97, 2286.
- Gong, K., Viboonkiat, R., Rehman, I.U., Buckton, G., Darr, J.A., 2005. Formation and characterization of porous indomethacin- PVP coprecipitates prepared using solvent-free supercritical fluid processing. *J Pharm Sci* 94, 2583–2590.
- Gryczke, A., Schminke, G.S., Maniruzzaman, M., Beck, J., Douroumis, D., 2011. Development and evaluation of orally disintegrating tablets (ODTs) containing ibuprofen granules prepared by hot melt extrusion. *Colloids Surf B Biointerfaces* 86, 275-84.
- Gupta, M.K., Tseng, Y-C., Goldman, D., Bogner, R.H., 2002. Hydrogen Bonding with Adsorbent during Storage Governs Drug Dissolution from Solid-Dispersion Granules. *Pharm Res* 19, 1663-72.
- Gupta, M.K., Vanwert, V., Bogner, R.H., 2003. Formation of Physically Stable Amorphous Drugs by Milling with Neusilin. *J Pharm Sci* 92, 536-51.
- Hasan, A., Peluso, C. R., Hull, T. S., Fieschko, J. and Chatterjee, S. G., 2013. A surface-renewal model of cross-flow microfiltration. *Brazilian Journal of Chemical Engineering*, 30, 167-186.
- He, X., Pei, L., Tong, H.H., Zheng, Y., 2011. Comparison of spray freeze drying and the solvent evaporation method for preparing solid dispersions of baicalein with Pluronic F68 to improve dissolution and oral bioavailability. *AAPS PharmSciTech* 12, 104-13.
- Jang, D.J., Sim, T., Oh, E., 2013. Formulation and optimization of spray-dried amlodipine solid dispersion for enhanced oral absorption. *Drug Dev Ind Pharm* 39, 1133-41.
- Koltuniewicz, A., and Noworyta, A., 1994. Dynamic properties of ultrafiltration systems in light of the surface renewal theory. *Ind Eng Chem Res* 33, 1771-1779.
- Kushida, I., Gotoda, M., 2013. Investigation for the amorphous state of ER-34122, a dual 5-lipoxygenase/cyclooxygenase inhibitor with poor aqueous solubility, in HPMC solid dispersion prepared by the solvent evaporation method. *Drug Dev Ind. Pharm* 39, 1582-8.
- Lang, B., McGinity, J.W., Williams III, R.O., 2014. Hot-melt extrusion – basic principles and pharmaceutical applications. *Drug Dev Ind Pharm* 40(9), 1133-55.

- Levenspiel, O., 1972. Chemical reaction engineering, 2nd Edition, Willey, USA.
- Maclean, J., Medina, C., Daurio, D., Alvarez-Nunez , F., Jona, J., Munson, E., Nagapudi, K., 2011. Manufacture and performance evaluation of a stable amorphous complex of an acidic drug molecule and neusilin. *J Pharm Sci* 100, 3332-44.
- Maniruzzaman, M., Boateng, J. S., Snowden, M.J., Douroumis, D., 2012. A review of hot-melt extrusion: process technology to pharmaceutical products. *ISRN Pharmaceutics* 2012, 436763.
- Maniruzzaman, M., Morgan, D.J., Mendham, A.P., Pang, J., Snowden, M.J., Douroumis, D., 2013b. Drug-copolymer intermolecular interactions in hot-melt extruded solid dispersions. *Int J Pharm* 443(1-2), 199-208.
- Maniruzzaman, M., Rana, M.M., Boateng, J.S, Mitchell, J.C., Douroumis, D., 2013a. Dissolution enhancement of poorly water-soluble APIs processed by hot-melt extrusion using hydrophilic polymers. *Drug Dev Ind Pharm* 39, 218-27.
- Mellaerts, R., Jammaer, J.A.G., Speybroeck, M.V., Chen, H., Humbeek, J.V., Augustijns, P., Mooter, G.V.D., Martens, J.A., 2008a. Physical State of Poorly Water Soluble Therapeutic Molecules Loaded into SBA-15 Ordered Mesoporous Silica Carriers: A Case Study with Itraconazole and Ibuprofen. *Langmuir* 24, 8651-8659.
- Mellaerts, R., Mols, R., Jammaer, J.A.G., Aerts, C.A., Annaert, P., H., Humbeek, J.V., Mooter, G.V.D., Augustijns, P., Martens, J.A., 2008b. Increasing the oral bioavailability of the poorly water soluble drug itraconazole with ordered mesoporous silica. *Eur J Pharm Biopharm* 69, 223–230.
- Neuslin® technical brochure; Fuji chemical industry co., ltd., Japan (www.neusilin.com): last accessed 10th March 2014.
- Repka, M. A., Shah, S., Lu, J., Maddineni, S., Morott, J., Patwardhan, K., Mohammed, N.N., 2012a. Melt extrusion: process to product. *Exp Opin Drug Deliv* 9(1), 105-25.
- Repka, M.A., Majumdar, S., Battu S.K., Srirangam, R., Upadhye, S.B., 2008. Applications of hot-melt extrusion for drug delivery. *Exp Opin Drug Deliv* 5(12), 1357-76.
- Repka, M.A., Shah, S., Lu, J., Maddineni, S., Morott, J., Patwardhan, K., Mohammed, N.N., 2012b. Melt extrusion: process to product. *Expert Opin Drug Deliv* 9(1), 105-25.

- Srinarong, P., DeWaard, H., Frijlink, H.W., Hinrichs, W.L., 2011. Improved dissolution behavior of lipophilic drugs by solid dispersions: the production process as starting point for formulation considerations. *Expert Opin Drug Deliv* 8, 1121-40.
- Sun, J., Wang, F., Sui, Y., She, Z., Zhai, W., Wang, C., Deng, Y., 2012. Effect of particle size on solubility, dissolution rate, and oral bioavailability: evaluation using coenzyme Q10 as naked nanocrystals. *Int. J Nanomedicines* 7 5733–5744.
- Tong, P., Taylor, L.S., Zografi, G., 2002. Influence of Alkali Metal Counterions on the Glass Transition Temperature of Amorphous Indomethacin Salts. *Pharm Res* 19 (5), 649-654.
- US pharmacopoeia, 2015a, http://www.pharmacopoeia.cn/v29240/usp29nf24s0_m40420.html; last accessed Sep 2015.
- US pharmacopoeia, 2015b (<http://www.usp.org/usp-nf/harmonization/monographs>); last accessed July 2015.
- Watanabe, T., Hasegawa, S., Wakiyama, N., Usui, F., Kusai, A., Isobe, T., Senna, M., 2002. Solid State Radical Recombination and Charge Transfer across the Boundary between Indomethacin and Silica under Mechanical Stress. *J Solid State Chem* 164(1), 27–33.

- **Figures caption list**

-

- Fig. 1** (a) Schematic diagram of HME processing ; (b) steps involved to manufacture extruded granules; (c) collected granules.
- Fig. 2** Residence time distribution and mean residence time data of IND/MAS 40% formulation.
- Fig. 3a** SEM images of IND/MAS 20% (a - c) and IND/MAS 40% (d- f) extruded formulations.
- Fig. 3b** Particle size distribution of extruded formulations processed via one-step extrusion processing.
- Fig. 4** Height (left) and Phase (right) of AFM images of a) 20%, b) 30%, c) 40% of IND/MAS extrudates.
- Fig. 5** XRPD diffractogram of IND pure (inset) and all IND/MAS

formulations.

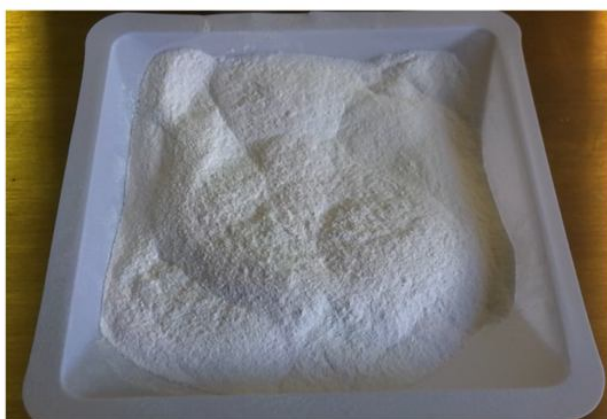
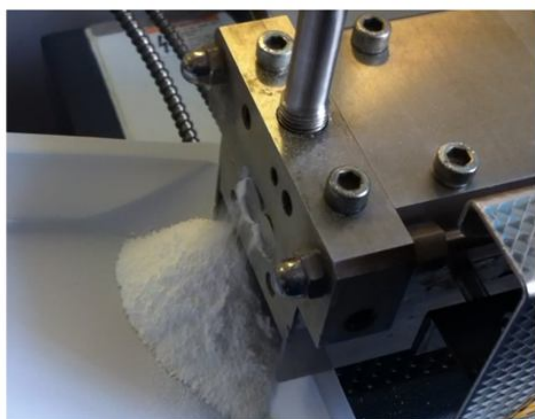
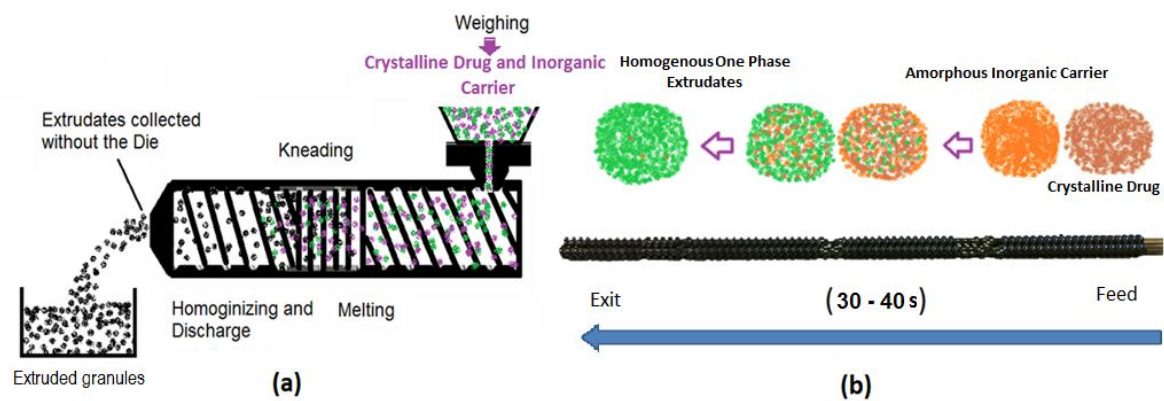
Fig. 6 a) DSC thermal transitions of IND/MAS 20-40% physical mixtures (PM) and extrudates (EXT), b) Thermal transitions of IND/MAS 40% formulations.

Fig. 7 FTIR spectra of bulk IND, MAS and extruded formulations (30-40%).

Fig. 8 IND release profiles, a) physical mixtures (PM) and b) extruded formulations (EXT). (n = 3, paddle speed 100 rpm at $37 \pm 0.5^\circ\text{C}$).

Table 1: DSC thermal transitions data of pure drug, physical mixtures and extrudates

Formulations	Glass transition/ enthalpy ($^\circ\text{C} / \Delta\text{H}, \text{Jg}^{-1}$)	Melting endotherm/ Enthalpy ($^\circ\text{C} / \Delta\text{H}, \text{Jg}^{-1}$)
IND	-	161.08/100.88
MAS	-	161.70/76.72
Physical mixtures (PM) and extruded formulations (EXT)		
	PM	EXT
	($^\circ\text{C} / \Delta\text{H}, \text{Jg}^{-1}$)	($^\circ\text{C} / \Delta\text{H}, \text{Jg}^{-1}$)
IND/MAS 20%	150.34/9.41	No transitions
IND/MAS 30%	151.86/19.01	No transitions
IND/MAS 40%	154.88/27.85	No transitions



(c)

Figure 1

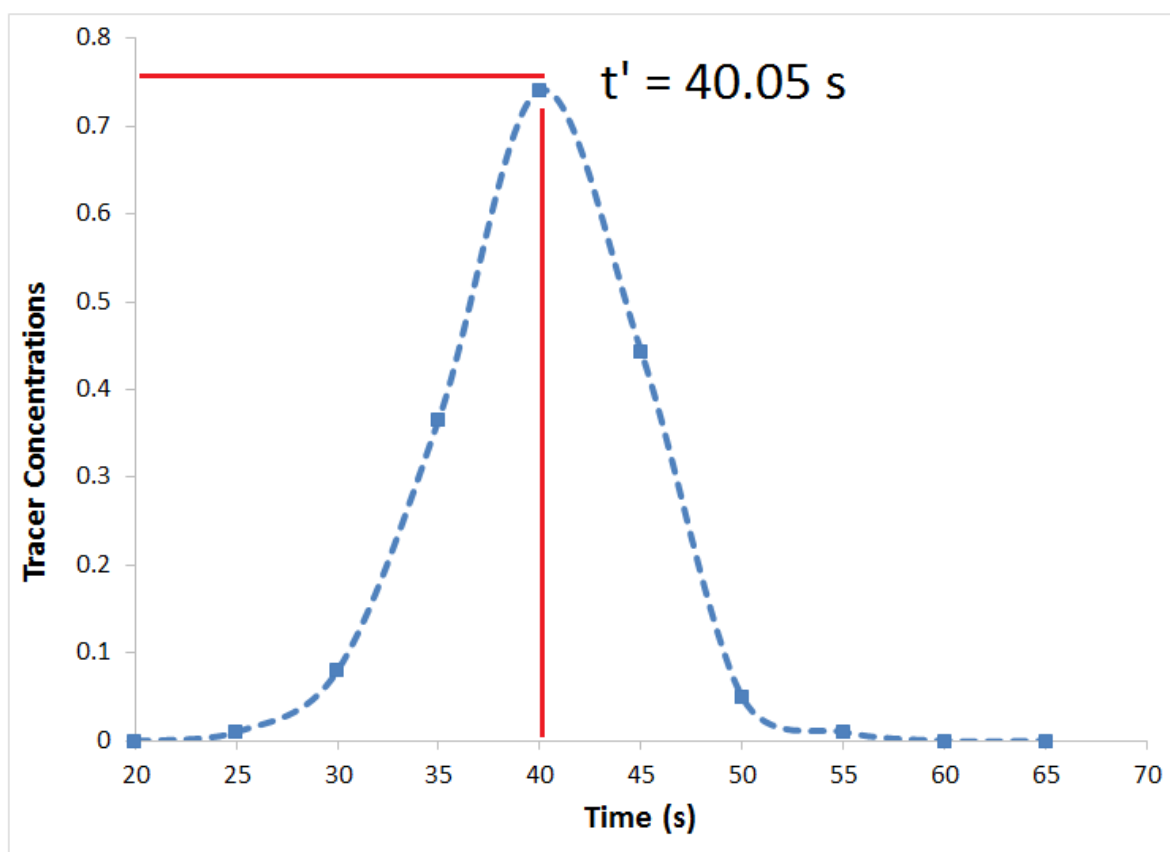


Figure 2

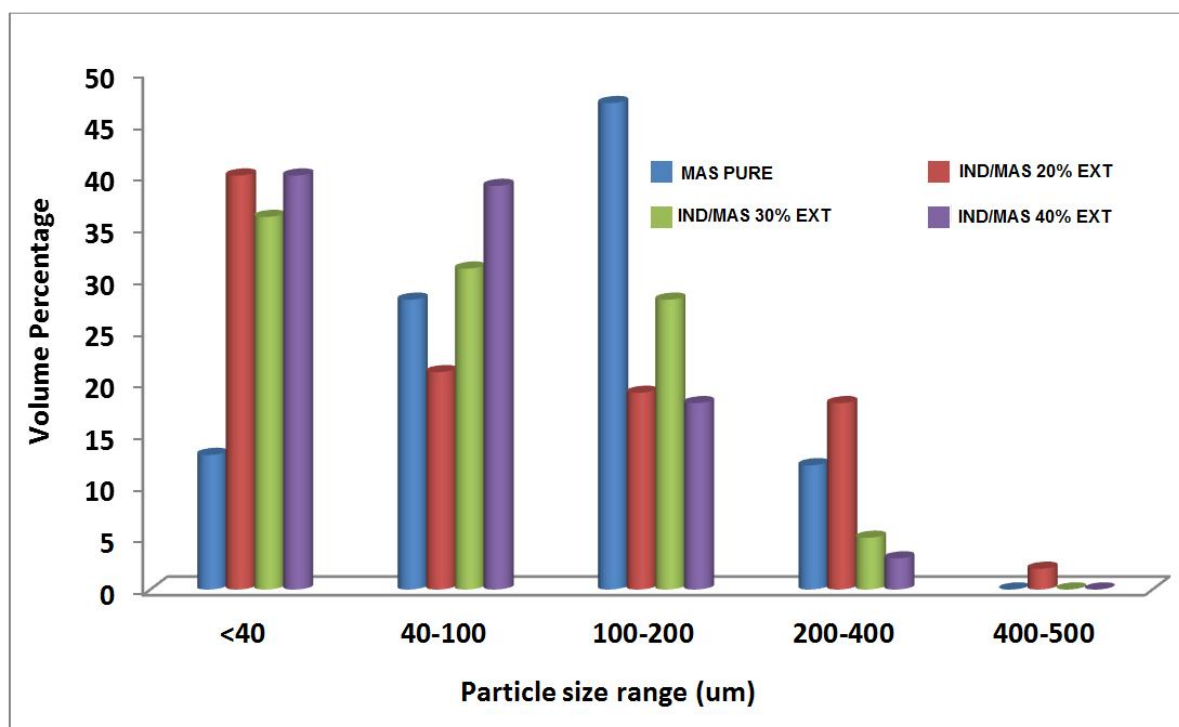
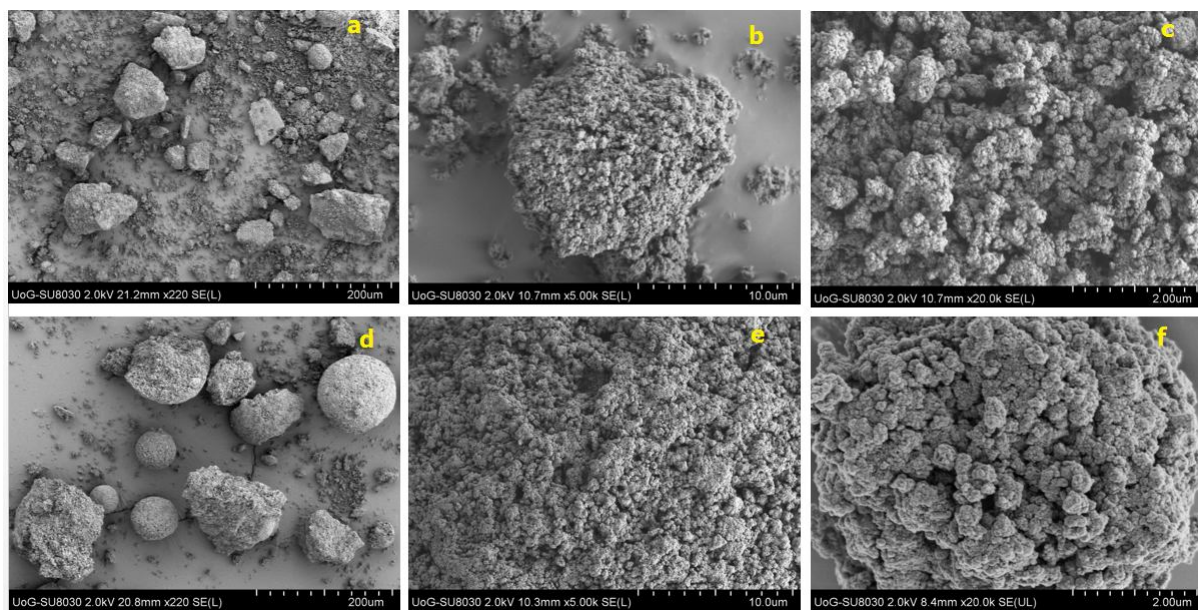


Figure 3

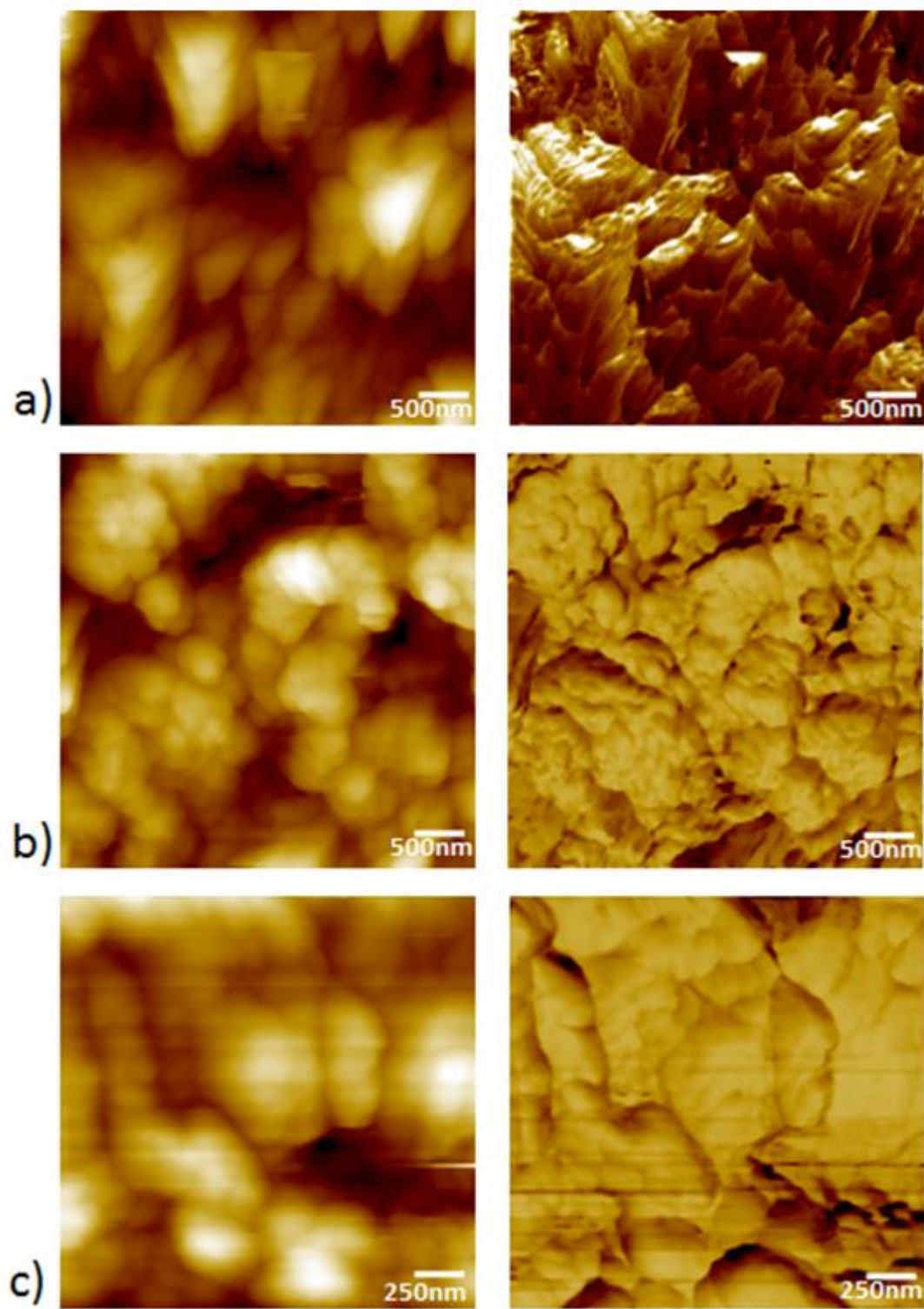


Figure 4

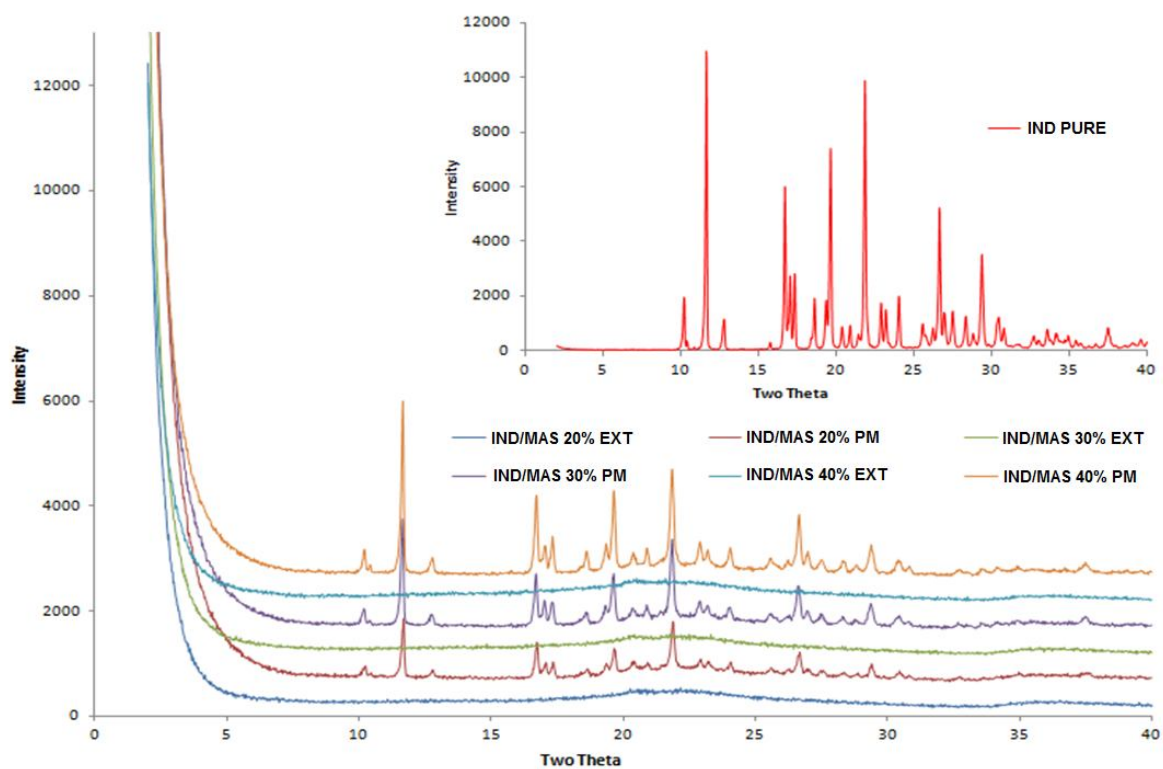


Figure 5

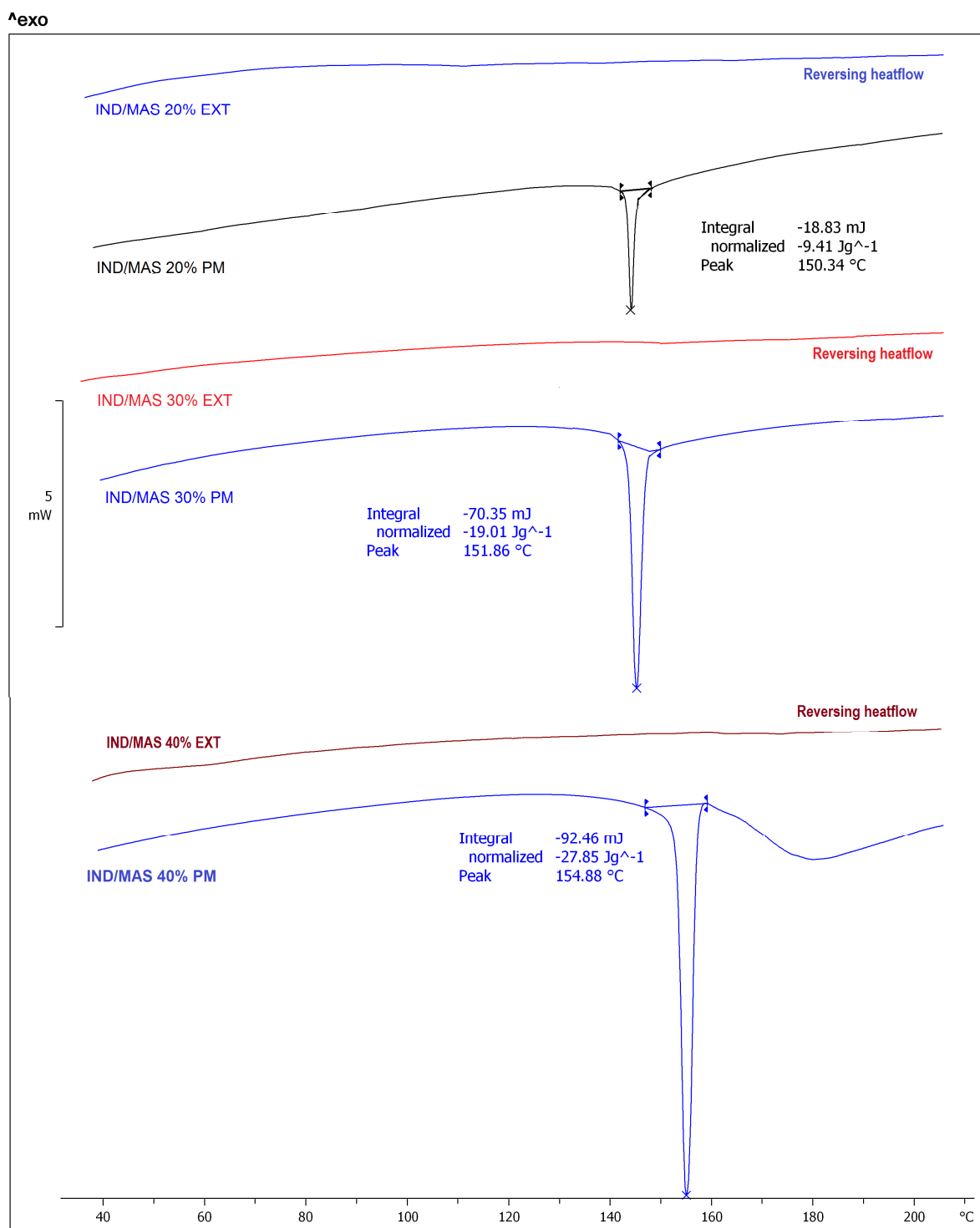


Figure 6

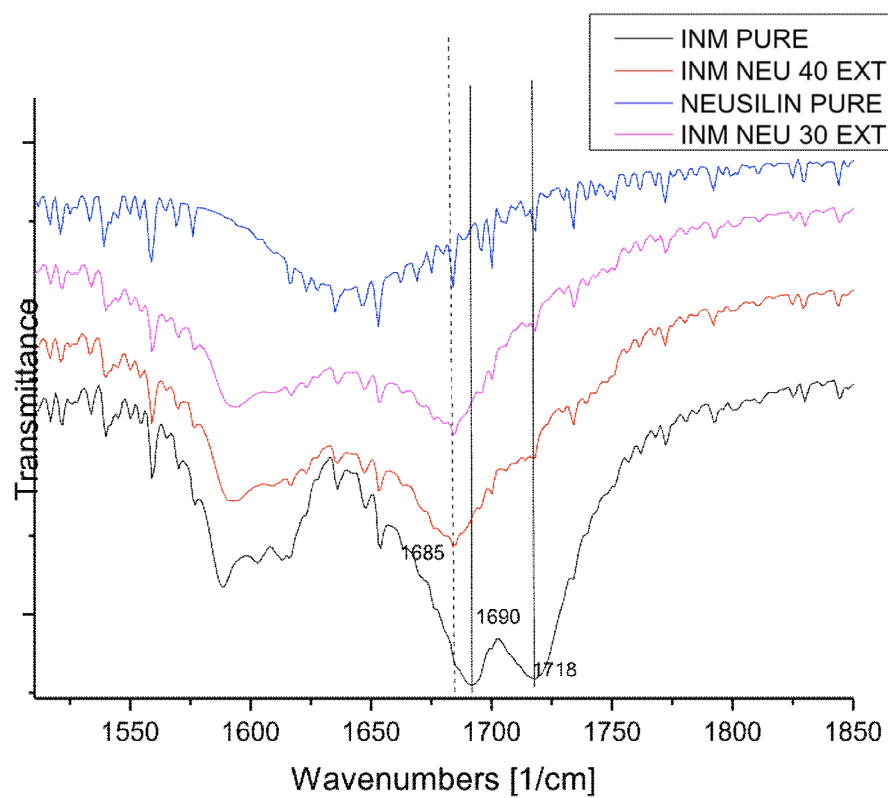


Figure 7

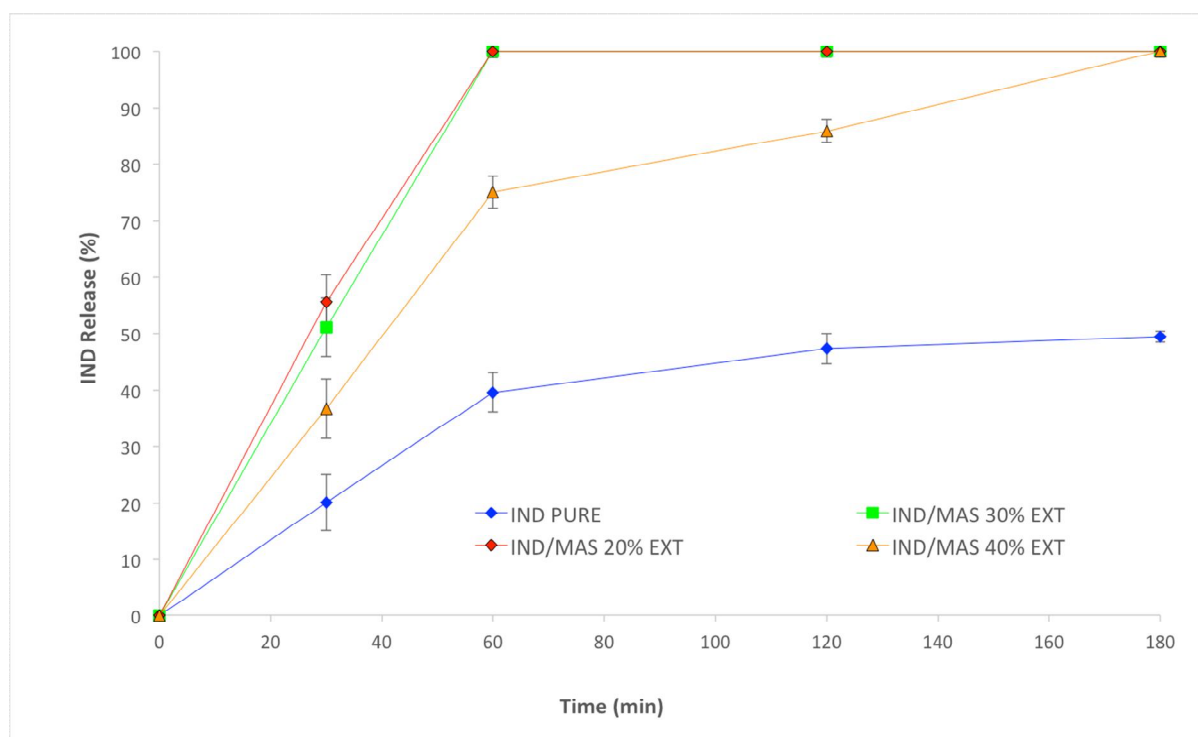
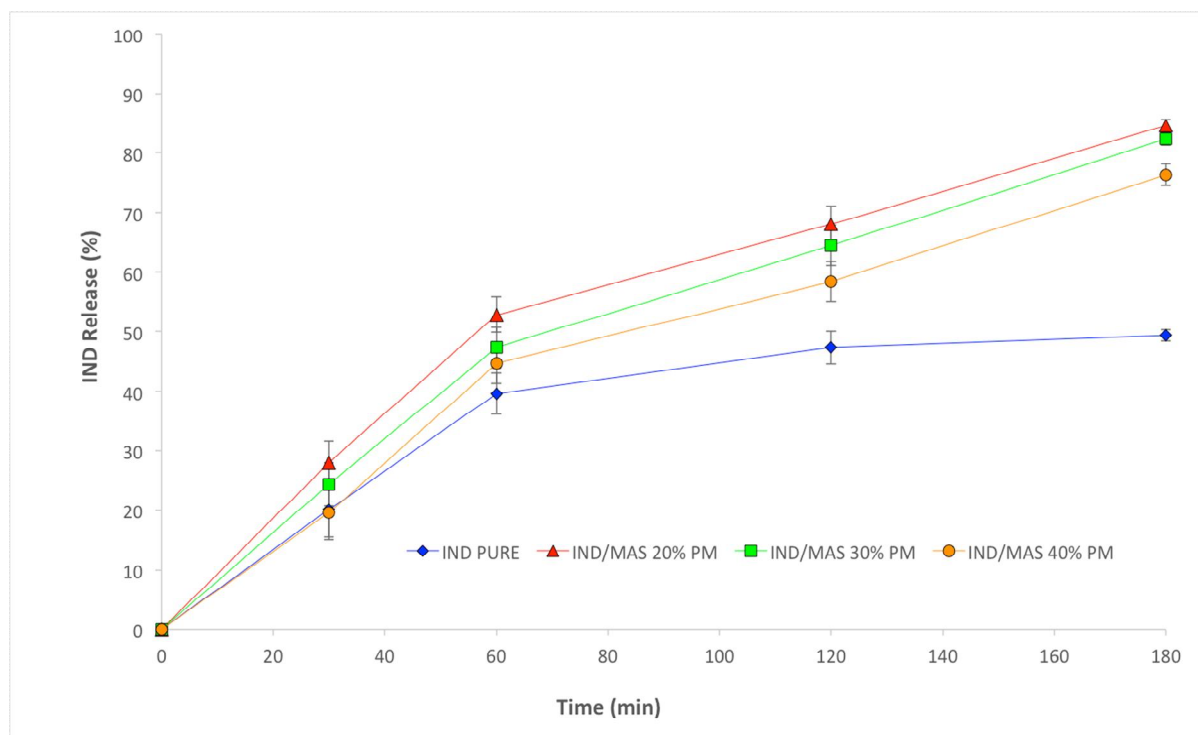


Figure 8